Investigation on carbonizing behaviors of nanometer-sized Cr_2O_3 particles dispersed on alumina particles by metalorganic chemical vapor deposition in fluidized bed

Hao-Tung Lin, Jow-Lay Huang,[a] Wen-Tse Lo
Department of Materials Science and Engineering, National Cheng-Kung University, Tainan 701, Taiwan, Republic of China
Wen-Cheng J. Wei
Department of Materials Science and Engineering, National Taiwan University, Taipei, Taiwan 106, Republic of China

(Received 30 October 2004; accepted 20 April 2005)

Nanoscaled Cr_2O_3 powder with an average particle size of 20–40 nm, coated on alumina particles, has been produced by means of chemical vapor deposition (CVD) in a fluidized chamber, using the pyrolysis of $Cr(CO)_6$ precursor. Amorphous and crystalline Cr_2O_3 particles were obtained when the temperatures of the pyrolysis were 300 and 400 °C, respectively. To prepare nanoscaled Cr_3C_2 powder from the nanometer-sized Cr_2O_3, carbonizing behavior of the Cr_2O_3 particles was investigated. It was found that, when amorphous Cr_2O_3 powders were carbonized in graphite furnace at 1150 °C for 2 h in vacuum (10^{-3} Torr), the powder was transformed into Cr_3C_2, while the crystalline Cr_2O_3 was transformed into a mixture of Cr_7C_3 and Cr_3C_2. The examinations by x-ray diffraction, transmission electron microscopy, and energy dispersive spectroscopy confirmed the transformation of the nano-sized Cr_3C_2 powders. The results of thermogravimetry and differential thermal analysis indicated that the transformation temperature was ~1089 °C for amorphous Cr_2O_3 and ~1128 °C for crystalline Cr_2O_3.

I. INTRODUCTION

Alumina has been broadly used in structural ceramic applications such as wear, cutting tools, balls, catalysts, spark plugs, etc. because of its excellent mechanical properties, good chemical stability, and high-temperature characteristics.[1,2] Its intrinsic brittleness and relatively poor reliability, however, made the improvement of the toughening of alumina ceramics to be an important and challenging area. The incorporation of secondary phases (e.g., particulates, fibers, or platelets) has been proven to be an easy, safe, and economical toughening technique for alumina ceramics.[3–5] Among those approaches, incorporating chromium carbide (Cr_3C_2) particles into Al_2O_3 matrix has been successfully achieved for toughening purposes.[6–9] Other materials such as SiC reinforced particles on Al_2O_3 composites mostly improve the mechanical properties, but the toughness enhancement (3.5 ~ 5.8 MPa.m$^{1/2}$) is not significant.[10–12] Therefore, to improve the toughness behavior, Cr_2O_3 dispersed in the alumina matrix (4.8–7.5 MPa m$^{1/2}$) was carbonized. The advantages of adding nanometer inclusions have been reported by Niihara to achieve several modifications,[10] such as the reduction of grain size of matrix grains, strengthening, and toughening.

When traditional mixing techniques are used for preparing particle-reinforced composites, nanoscale reinforcing particles are difficult to uniformly disperse on the micro-scale matrix particles. This problem is ascribed to the fact that nano-sized particles easily agglomerate due to the interaction between the particles.[13] The agglomeration will promote the generation of voids during the densification and microstructual inhomogeneity.[14]

It has been found that the combination of conventional fluidized bed technology with chemical vapor deposition (CVD) is an effective method to deposit particles.[15–18] It was recognized that fluidized bed reactor could supply such an environment with uniform temperature and concentration of the coating precursor, which can provide the possibility of good dispersion of the nanoparticles on the matrices.[19]

In this work, coating nanometer-sized Cr_2O_3 on micrometer-sized Al_2O_3 was accomplished by metalorganic chemical vapor deposition (MOCVD) in a fluidizing reactor using $Cr(CO)_6$ as the precursor. Carbonizing

[a]Address all correspondence to this author.
e-mail: JLH888@mail.ncku.edu.tw
DOI: 10.1557/JMR.2005.0268

behavior of the nanometer-sized Cr_2O_3 and the formation reactions of Cr_3C_2 and Cr_7C_3 during carbothermal reduction process of the Cr_2O_3 were investigated.

II. EXPERIMENTAL

In the MOCVD process, the precursor to form Cr_2O_3 was chromium hexacarbonyl [$Cr(CO)_6$, 99%, Strem Chemicals Co., USA]. Al_2O_3 powder with the average size of about 0.7 μm (A16-SG, Alcoa) was used as matrix powder. The vapor of the precursor was carried by He gas (99.9% pure) introduced into a fluidized bed reactor for the MOCVD process.

Based on Lander's results,[20] the precursor container was therefore kept at 75 °C in vacuum (10 t) in the present tests. To investigate the influence of the temperature on the product deposited on the fluidizing Al_2O_3 particles, the $Cr(CO)_6$ vapor was decomposed in the fluidized chamber at 300 and 400 °C, respectively. The apparatus consisted of six main components: gas supply, MOCVD precursor, fluidized bed reactor, power supply, temperature controller, cold trap, and vacuum system, as shown schematically in Fig. 1.

The pressure in the chamber was measured with a pressure meter. A rotary vacuum pump was set up with a cold trapping system. The temperature controllers (TC) were connected to a heating system that controlled the temperature of the fluidized reactor and precursor container.

The carbothermal treatment of the prepared Cr_2O_3/Al_2O_3 powders was first performed in a graphite furnace operating at 1150 °C for 2 h under vacuum conditions (10^{-3} Torr).

The deposited particles were analyzed by x-ray diffraction (XRD; Rigaku D/MaxII, Japan), and transmission electron microscopy (TEM; Hitachi FE-2000, Japan) equipped with energy dispersive x-ray spectroscopy (EDS; UK) to identify the phase composition and morphology. X-ray photoelectron spectroscopy (XPS; VG Scientific 210, UK) was used to determine the coating phases by binding energy. A Brunauer–Emmett–Teller (BET) instrument (Micromeritics Gemini 2360, USA) was used to measure the specific surface area by nitrogen adsorption, and C/O analyzer (LECO CS-244, USA) was used to measure the carbon content of coated powder by a combustion method. Differential thermal analysis/thermogravimetry (DTA/TG; GravitNERZSCH STA 409 PC, Germany) was used to investigate the reacting temperature of Cr_2O_3-graphite mixtures.

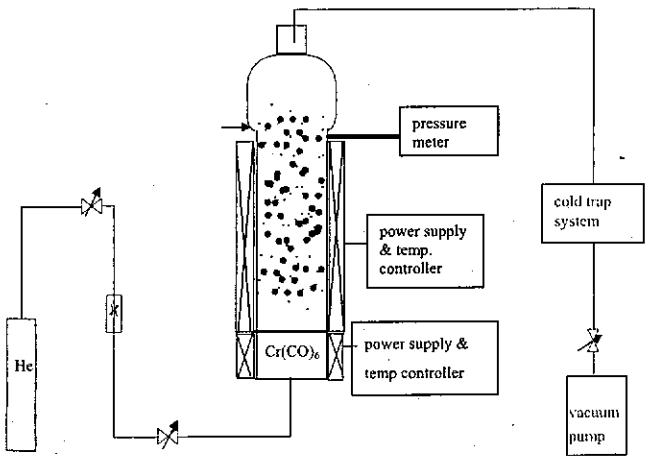

FIG. 1. Schematic diagram of MOCVD and fluidized bed.

III. RESULTS AND DISCUSSION

Figure 2 shows the TEM micrograph of as-deposited powder prepared at 300 °C for 2 h in fluidized bed. The nanometer-sized particles (~30 nm) coated and dispersed uniformly on an alumina particle were observed in Fig. 2(a). Figure 2(b) is the EDS spectrum of the coating particle (marked by A) in Fig. 2(a), which clearly reveals the composition of C, Cr, and O elements. The Cu intensity coming from Cu grid and the Al from the matrix were also detected. The EDS results showed the evidence that the particles resulted from the pyrolysis of the Cr precursor.

Figures 3 and 4 display XPS spectra of the Cr2*p* and C1*s* regions of the as-deposited powder prepared at 300 °C. Figure 3 shows two peaks corresponding to the spin-orbit splitting $2p_{1/2}$ (left) and $2p_{3/2}$ (right) of Cr, which have bonding energies of 586.3 and 576.6 eV, respectively. The band shift of these two peaks is 9.7 eV, which is in good agreement with previously reported data[21] and confirms the existence of Cr_2O_3 particles in the as-deposited powder. The XPS spectra of the C1*s* regions in Fig. 4 provide the evidence for which at least two forms of carbon in the as-deposited powder exist. One is free carbon (C–C) at 284.6 eV, and the other carbon bonded to chromium atoms (C–Cr) at 283.5 eV.

Figure 5(a) is the TEM diffraction pattern of as-deposited powder fabricated at 300 °C. Figures 5(b) and 5(c) are the TEM diffraction patterns of the as-deposited powder fabricated at 400 °C. Figure 5(a) demonstrates an amorphous phase of the as-deposited particles. Figures 5(b) and 5(c) show two types of crystalline particles in the as-deposited powder: Cr_2O_3 phase with hexagonal structure and CrC_{1-x} phase with NaCl (B1) structure.[22] These results are similar to the finding by Schuste et al.[23] They reported the CrC_{1-x} phase and free carbon were fabricated in the coating when $Cr(CO)_6$ was used as the precursor for the MOCVD process. Bouzy and coworkers[22] have reported that nonstoichiometric CrC_{1-x} was a metastable phase and deduced that small C atoms were inserted in the octahedral interstitial sites of the cubic-close Cr packings in this structure. From the report by

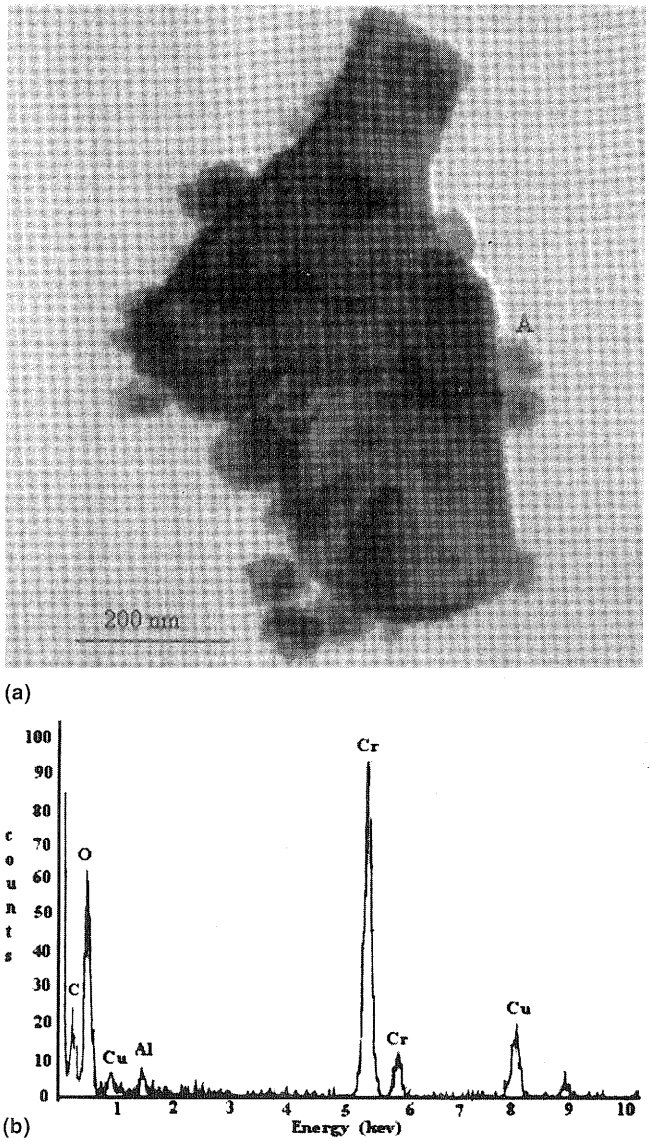

FIG. 2. (a) TEM micrograph of nanometer-sized particles dispersed on alumina particles prepared at 300 °C in a fluidized bed for 2 h. (b) EDS spectrum of the coating particle A in (a).

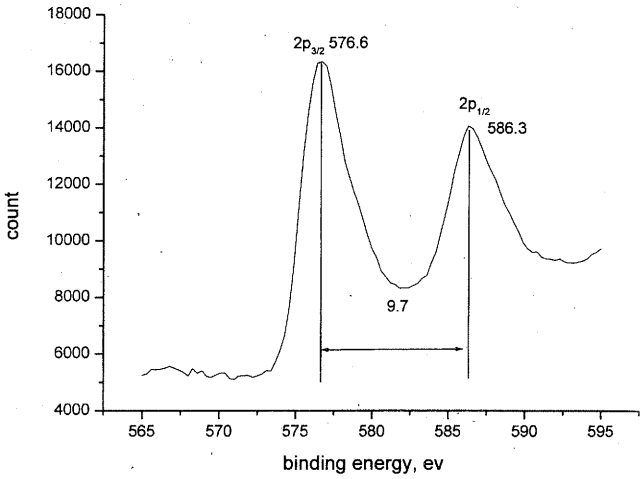

FIG. 3. X-ray photoelectron spectra of the Cr 2*p* regions of as-deposited composite powders prepared at 300 °C in fluidized bed.

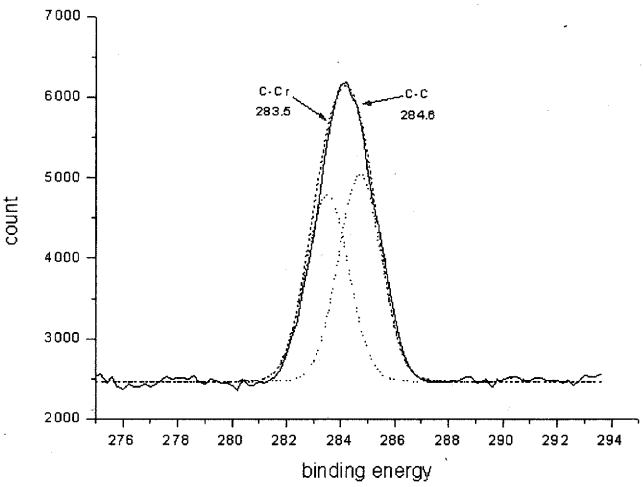

FIG. 4. X-ray photoelectron spectra of the C1*s* regions of as-deposited composite powder prepared at 300 °C in fluidized bed.

Bewilogua and collaborators,[24] this NaCl (B1) structure was also observed in Cr–C films prepared by ion-plating.

According to the literature,[25] Cr_3C_2 has higher oxidation resistance than Cr_7C_3, which begin to oxidize at 1000 and 800 °C, respectively. Due to the fact that the hardness of Cr_7C_3 is higher than that of Cr_3C_2, Cr_3C_2 has a better toughening effect. Figure 6 shows the TEM diffraction patterns of the 300 and 400 °C powders treated at 1150 °C in graphite furnace under vacuum (10^{-3} Torr) for 2 h. Although the particles obtained at 300 °C by fluidized reactor are in an amorphous phase, as shown in Fig. 5(a), it could be changed to crystalline Cr_3C_2 after thermal treatment. The diffraction pattern of the 300 °C shown in Fig. 6(a) was expected so that the phase was orthorhombic Cr_3C_2. In contrast, the thermal treatment of the crystalline particles obtained at 400 °C yields a mixture of crystalline orthorhombic Cr_3C_2 and hexagonal Cr_7C_3 particles evident by their TEM diffraction patterns displayed in Figs. 6(b) and 6(c). The difference in the phase composition between the particles in Fig. 6 was further examined by the XRD technique (results shown in Fig. 7). Figures 7(a) and 7(b) are the XRD patterns of the 300 and 400 °C powders that underwent the thermal treatment. Figure 7(b) shows that the peaks of Cr_7C_3 particles are accompanied by Cr_3C_2 peaks when the initial particles were treated at 400 °C fluidized bed, while only Cr_3C_2 existed in the powders prepared at 300 °C, as shown in Fig. 7(a). Similar phase transformations have been explained previously by other researchers.[26–29]

Chu et al.[26] reported that a carbon with higher activity could promote formation of Cr_3C_2 by Cr_2O_3. Direct contact between the graphite and Cr_2O_3 particles during

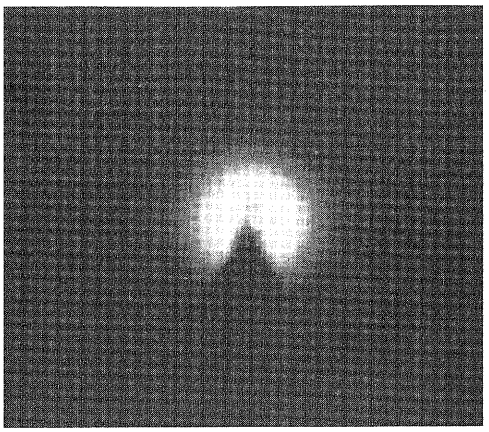

(a)

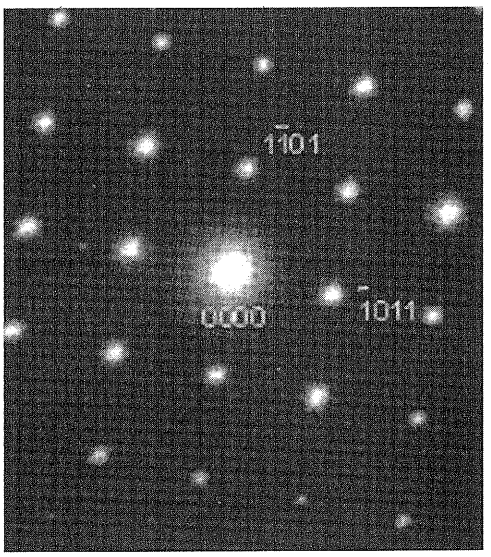

(b)

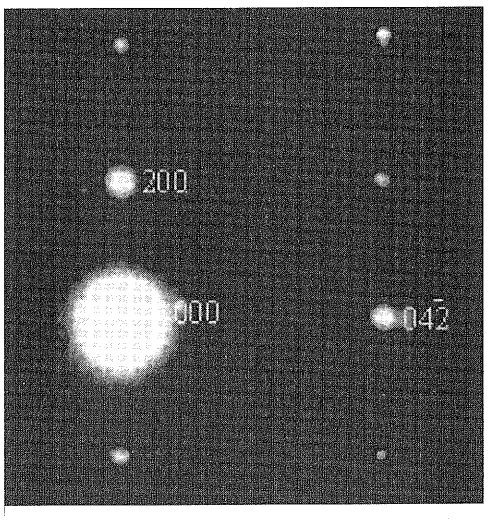

(c)

FIG. 5. TEM diffraction patterns of the coated particles (a) prepared at 300 °C in fluidized bed, showing amorphous phase and (b, c) prepared at 400 °C in fluidized bed. (b) Cr_2O_3 phase with hexagonal structure and (c) CrC_{1-x} phase with NaCl (B1) structure, respectively.

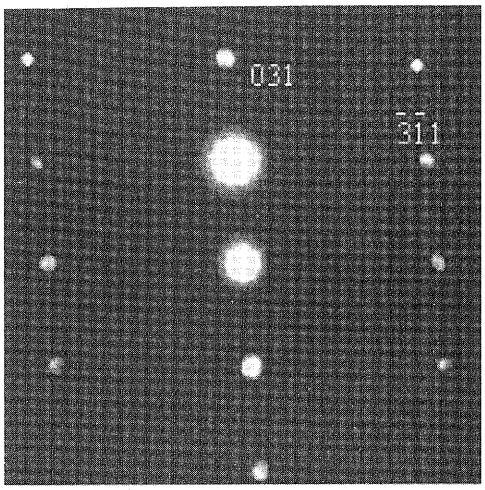

(a)

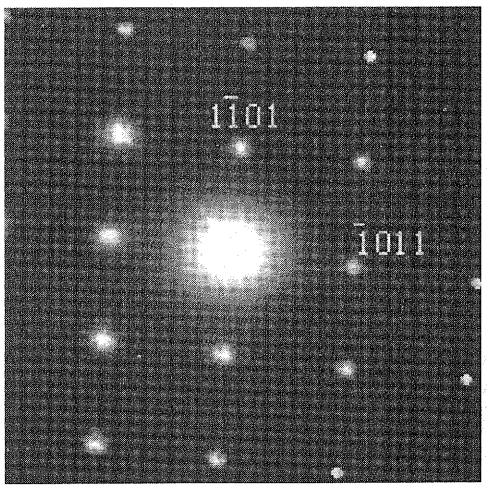

(b)

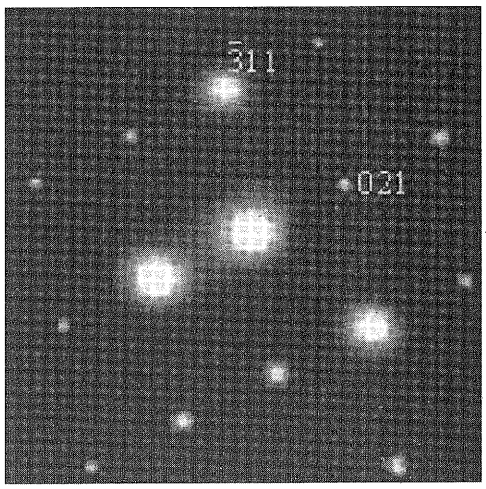

(c)

FIG. 6. TEM diffraction patterns of the (a) 300 °C powder treated at 1150 °C in graphite furnace under vacuum for 2 h, showing Cr_3C_2 phase with orthorhombic structure. (b, c) 400 °C powder treated under same thermal treatment condition, showing Cr_7C_3 phase with hexagonal structure and Cr_3C_2 phase with orthorhombic structure, respectively.

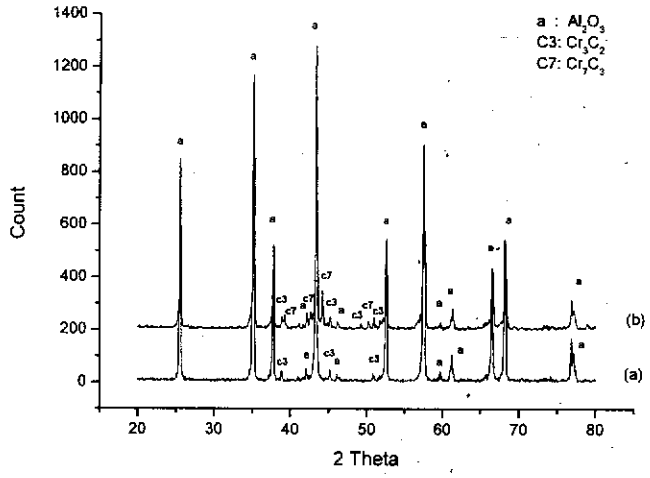

FIG. 7. XRD patterns of the (a) 300 °C and (b) 400 °C as-deposited powders after thermal treatment in graphite furnace at 1150 °C for 2 h in vacuum.

TABLE I. Specific surface area and carbon content of specimens.

Item	Fabricated in fluidized reactor	Carbon content (%)	BET surface area (m^2/g)
1	300 °C, 2 h	0.75	25.5
2	400 °C, 2 h	0.23	11.2

thermal treatment led to a higher probability of Cr_3C_2 particle formation due to its higher carbon activity. Otherwise a Cr_7C_3 phase would be generated during the carbonizing process. Hernandez and coworkers[27] found that the graphite mold introduced carbon into the powders and transformed the Cr_2O_3 into Cr_7C_3 when a thermal treatment was carried out in a graphite furnace. Berger et al.[28] and Antony et al.[29] also reported that the Cr_3C_2 phase was initially generated in the interface region between Cr_2O_3 and C, followed by an interface shift slowly toward the center of the particle. It is therefore a reasonable speculation that nanometer-sized Cr_2O_3 results in higher possibility of transformations of the Cr_3C_2 phase than larger sized Cr_2O_3 particles do. From those results, one can learn that free C plays an important role in the transformation. More carbon in contact with Cr_2O_3 had generated more Cr_3C_2. In this work, Table I indicates the as-deposited amorphous powder prepared at 300 °C had more free carbon than the crystalline powders prepared at 400 °C. This was probably because the former had specific surface area (25.5 m^2/g) larger than the latter (11.2 m^2/g). A higher content of free carbon and C–Cr species shown in Fig. 4 was trapped in the 300 °C powder and led to the formation of monolithic Cr_3C_2.

In the case of the metastable CrC_{1-x} phase, according to the results of Bewilogua and collaborators,[24] an annealing treatment would cause the transformation of the CrC_{1-x} into the stable Cr_3C_2. The C–Cr species first became the CrC_{1-x} structure and then transferred into the

TABLE II. Compositions of mixture 1 and mixture 2 used in the TG/DTA experiments.

Mixture no.	Composition
1	1 mol powder fabricated at 300 °C without adding Al_2O_3 particles; 4.33 mol graphite powder
2	1 mol powder fabricated at 400 °C without adding Al_2O_3 particles; 4.33 mol graphite powder

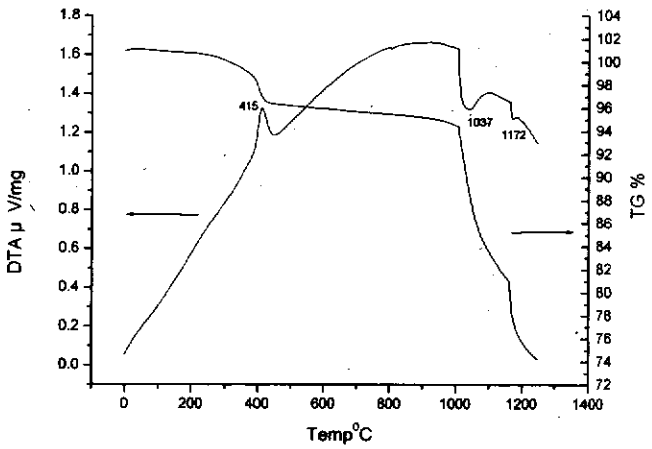

FIG. 8. TG/DTA diagrams of mixture 1.

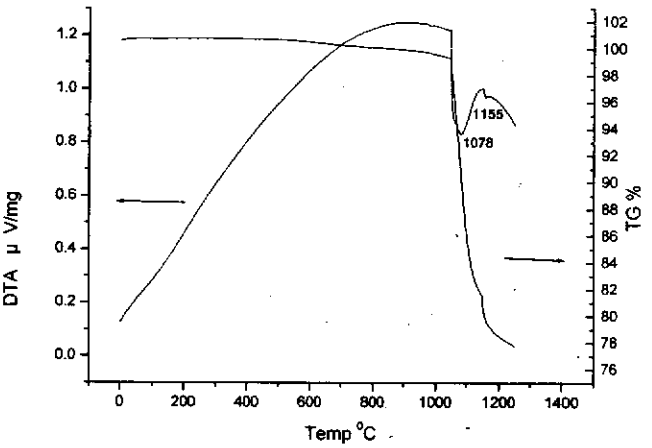

FIG. 9. TG/DTA diagrams of mixture 2.

Cr_3C_2 in subsequent thermal treatment. Therefore, it was reasonable for 400 °C powder to form simultaneously the Cr_3C_2 and Cr_7C_3 phases because the amount of the free carbon and C–Cr species in 400 °C powder was not enough to transfer to monolithic Cr_3C_2.

To avoid the catalytic effects of Al_2O_3 matrix, the powders processed at 300 and 400 °C were also collected without adding Al_2O_3 particles. Table II displays the compositions of the samples, denoted by "mixture 1" and "mixture 2." The ratio (1:4.33 mol) of powders and graphite was selected according to Eq. (2). Figures 8 and 9 show the TG/DTA diagrams of the mixtures. The DTA

curve in Fig. 8 shows an exothermic peak with a maximal reaction at 415 °C and begins at ~400 °C. It is consistent with the result that reveals the coating particle obtained at 400 °C has crystalline Cr_2O_3 phase. The mass loss shown in the TG curves is because of the production of CO gas during the heating process.

The formations of Cr_3C_2 and Cr_7C_3 can be described by the following equations

$$3\,Cr_2O_{3(s)} + 13\,C_{(s)} \rightarrow 2\,Cr_3C_{2(s)} + 9\,CO_{(g)} \quad , \quad (1)$$

$$7\,Cr_2O_{3(s)} + 27\,C_{(s)} \rightarrow 2\,Cr_7C_{3(s)} + 21CO_{(g)} \quad . \quad (2)$$

According to the results of Berger et al.,[28] Eq. (1) describes the main reaction in the temperature range of 1050–1150 °C. However, in the temperature range of 1150–1250 °C, the main reaction is described by Eq. (2). The two endothermic peaks in DTA curves correspond to the formation of Cr_3C_2 and Cr_7C_3 phases. Figures 8 and 9 indicate that the formation temperature of Cr_3C_2 in mixture 1 (1037 °C) was lower than mixture 2 (1078 °C), whereas the formation temperature of Cr_7C_3 in mixture 1 (1172 °C) was higher than mixture 2 (1155 °C). The fact that the amorphous Cr_2O_3 in mixture 1 had higher content of free carbon contacted with Cr_2O_3 particles and Cr–C species promoted the formation of Cr_3C_2 at lower temperature. Nevertheless, the crystalline Cr_2O_3 had fewer carbon species, which helped the formation of Cr_7C_3 at lower temperature.

IV. CONCLUSIONS

The amorphous powder fabricated at 300 °C in fluidized bed was transformed into Cr_3C_2 in graphite furnace at 1150 °C for 2 h in vacuum, while the crystalline powder prepared at 400 °C in fluidized bed transferred to a mixture of Cr_3C_2 and Cr_7C_3 in same treatment condition. This difference was due to the amorphous Cr_2O_3 powders contained more free carbon and C–Cr species than that of the crystalline Cr_2O_3 powder, which formed CrC_{1-x} phase at 400 °C and became Cr_3C_2 after thermal treatment.

The amorphous as-deposited powder, with higher carbon content had greater specific surface area and higher activity, which consequently promoted the formation of Cr_3C_2 at lower temperature. In addition, the crystalline phase had fewer amounts of carbon species and lower specific surface area due to the crystalline structure, which helped the formation of Cr_7C_3 at lower temperature.

ACKNOWLEDGMENT

The authors would like to thank National Science Council of the Republic of China for its financial support under Contract No. NSC-92-2216-E-006-011.

REFERENCES

1. Y. Wang and S.M. Hsu: The effects of operating parameters and environment on the wear and wear transition of alumina. *Wear* **195,** 90 (1996).
2. B.B. Ghate, W.C. Smith, C.H. Kim, D.P.H. Hasselman, and G.E. Kane: Effect of chromia alloying on machining performance of alumina ceramic cutting tools. *Ceram. Bull.* **54,** 210 (1975).
3. S. Lio, M. Watanabe, M. Matsubara, and Y. Matsuo: Mechanical properties of alumina/silicon carbide whisker composites. *J. Am. Ceram. Soc.* **72,** 1880 (1989).
4. W.J. Tseng and P.D. Funkenbusch: Microstructure and densification of pressureless-sintered Al_2O_3/Si_3N_4. *J. Am. Ceram. Soc.* **75,** 1171 (1992).
5. Y.S. Chou and D.J. Green: Silicon carbide platelet/alumina composites: I. Effect of forming technique on platelet orientation. *J. Am. Ceram. Soc.* **75,** 3346 (1992).
6. C.T. Fu, J.M. Wu, and A.K. Li: Microstructure and mechanical properties of Cr_3C_2 particulate reinforced Al_2O_3 matrix composites. *J. Mater. Sci.* **29,** 2671 (1994).
7. J.L. Huang, Ho-Don Lin, Ching-An Jeng, and D.F. Lii: Crack growth resistance of Cr_3C_2/Al_2O_3 composites. *Mater. Sci. Eng.* **A279,** 81 (2000).
8. J.L. Huang, K.C. Twu, D.F. Lii, and A.K. Li: Investigation of Al_2O_3/Cr_3C_2 composites prepared by pressureless sintering (part 2). *Mater. Chem. Phys.* **51,** 211 (1997).
9. D.F. Lii, J.L. Huang, J.H. Huang, and H.H. Lu J: The interfacial reaction in Cr_3C_2/Al_2O_3 composites. *J. Mater. Res.* **14,** 817 (1999).
10. K. Niihara: New design concept of structural ceramics-ceramic nanocomposites. *J. Ceram. Soc. Jpn.* **99,** 974 (1991).
11. M. Sternitzke: Review: Structural ceramic nanocomposites. *J. Eur. Ceram. Soc.* **17,** 1061 (1997).
12. C.C. Anya: Microstructural nature of strengthening and toughening in Al_2O_3–SiC(*p*) nanocomposites. *J. Mater. Sci.* **34,** 5557 (1999).
13. G.Y. Onada, Jr. and L.L. Hench: *Ceramic Processing before Firing* (Wiley, New York, 1978), pp. 357–376.
14. E.A. Pugar and P.E.D. Morgan: Coupled grain growth effects in Al_2O_3/10 vol% ZrO_2. *J. Am. Ceram. Soc.* **69,** C120 (1984).
15. Y. Zhu, Y. Qian, and M. Zhang: γ-radiation synthesis of nanometer-size amorphous Cr_2O_3 powders at room temperature. *Mater. Sci. Eng. B* **41,** 294 (1996).
16. C.L. Chen and W.C. Wei: Sintering behavior and mechanical properties of nano-sized Cr_3C_2/Al_2O_3 composites prepared by MOCVI process. *J. Eur. Ceram. Soc.* **22,** 2883 (2002).
17. B.J. Wood, A. Sanjurjo, G.T. Tong, and S.E. Swider: Coating particles by chemical vapor deposition in fluidized bed reactors. *Surf. Coat. Technol.* **49,** 228 (1991).
18. K. Tsugeki, T. Kato, Y. Koyanagi, K. Kusakabe, and S. Morooka: Electronductivity of sintered bodies of α–Al_2O_3–TiN composite prepared by CVD reaction in a fluidized bed. *J. Mater. Sci.* **28,** 3168 (1993).
19. D. Kunii and O. Levenspiel: *Fluidization Engineering* (Huntington, NY, 1977), pp. 195–223.
20. J.J. Lander and L.H. Germer: Plating molybdenum, tungsten, and chromium by thermal decomposition of their carbonyls. *Am. Inst. Min. Metal. Eng. Technol.* **14**(6), 1 (1947).
21. C.D. Wagner, W.M. Riggs, L.E. Davis, and J.F. Moulder: *Handbook of X-ray Photoelectron Spectroscopy* (Perkin-Elmer, Minnesota, MN, 1979), p. 77.
22. E. Bouzy, E. Bauer-Grosse, and G. Le Caer: NaCl and filled Re_3B-type structures for two metastable chromium carbides. *Philos. Mag. B* **68,** 619 (1993).

23. F. Schuste and F. Maury: Influence of organochromium precursor chemistry on the microstructure of MOCVD chromium carbide coatings. *Surf. Coat. Technol.* **43,** 185 (1990).
24. K. Bewilogua, H-J. Heinitz, B. Rau, and S. Schulze: A chromium carbide phase with B1 structure in thin film prepared by ion plating. *Thin Solid Films* **167,** 233 (1988).
25. K.S. Edmund: *The Refractory Carbides,* Refractory Materials, Vol. 2 (Academic Press, New York and London, 1967), pp. 102–112.
26. W.F. Chu and A. Rahmel: The conversion of chromium oxide to chromium carbide. *Oxid. Met.* **15,** 331 (1981).
27. M.T. Hernandez, M. González, and A. De Pablos: C-diffusion during hot press in Al_2O_3–Cr_2O_3 system. *Acta Mater.* **51,** 217 (2003).
28. L-M. Berger, S. Stole, W. Gruner, and K. Wetzig: Investigation of the carbothermal reduction process of chromium oxide by micro- and lab-scale methods. *Int. J. Refract. Met. Hard Mat.* **19,** 109 (2001).
29. M.P. Antony, R. Vidhya, C.K. Mathews, and U.V. Varada Raju: Studies on the kinetics of the carbothermic reduction of chromium oxide using the evolved gas analysis technique. *Thermochim. Acta* **262,** 145 (1995).